

Cross Section Ratios for Elastic Proton Scattering

S. Austin, E. Kashy, C. King, R. Markham,
S. Motzny, and I. Redmount

We are using a novel technique to measure the ratios of cross sections for scattering of protons from the isotopes of a given element. The technique is to prepare a mixed target of the isotopes and then to separate scattering from different isotopes by their different kinematic shifts. This is simple at backward angles but, of course, the resolution requirements become more and more severe as one approaches $\theta=0^\circ$.

As a test case for this technique we have measured the scattering of 30.3 MeV protons from a metallic mixed Ca target in the angular range 19-125°. The 100 $\mu\text{g}/\text{cm}^2$ target was prepared by evaporating a mixture of approximately equal parts of the carbonates of ^{40}Ca , ^{44}Ca and ^{48}Ca . The relative abundance of each isotope in the target is currently being determined by Coulomb scattering of ^{16}O and ^{12}C ions. Scattered protons were detected by a slanted electrode proportional counter in the focal plane of the Enge spectrograph. A spectrum is shown in Fig. 1. The resolution of about 8 keV permits relatively reliable separation of peaks to $\theta \approx 20^\circ$. For $\theta \geq 40^\circ$ the accuracy of the ratios may be as good as $\pm(1-2\%)$. We are presently analyzing these data to obtain the ratios by using line shapes obtained from scattering by ^{40}Ca targets of the same thickness.

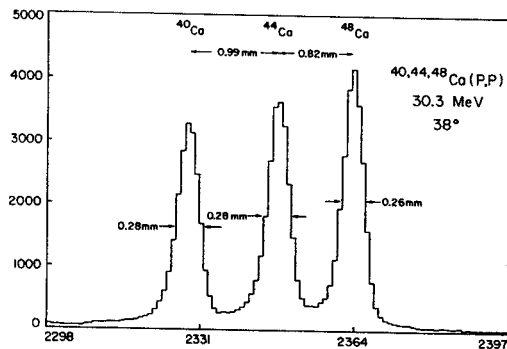


Fig. 1.--Spectrum of 30.3 MeV protons scattered at 38° from a target consisting of roughly equal parts of ^{40}Ca , ^{44}Ca and ^{48}Ca . The peak width of about 0.28 mm corresponds to an energy resolution of about 8.5 keV FWHM.

Our initial theoretical analysis will probably be based on optical model parameters¹ which fit the 30.3 MeV ^{40}Ca data obtained at the Rutherford Laboratory. Parameters of the potential which must be added to the ^{40}Ca potential to fit our ratios will be determined in a fitting procedure. Eventually we hope to use the "model independent" techniques for this purpose.

1. V. Hnizdo, O. Karban, J. Lowe, G.W. Greenlees and W. Makofske, Phys. Rev. **C3**, 1560 (1971) and references therein.

Most of the best neutron elastic data available is for neutron energies less than about 20 MeV, while most of the best proton data is at proton energies above 20 MeV. The MSU neutron time-of-flight (TOF) facility offers a nearly monoenergetic beam of neutrons from 25 MeV to 45 MeV. We are developing a system to obtain neutron elastic scattering data with uncertainties better than a few percent at forward angles. Neutron elastic angular distributions from isotopic targets over a substantial range of mass (primarily from ^{40}Ca to ^{209}Bi) and at several energies will be measured. Some preliminary $\sigma(\theta)$ have been measured for natural Fe(n,n) with $E_n=26$ MeV (Fig. 1) and for ^{40}Ca (n,n) with $E_n=30.3$ MeV (Fig. 2). The results are being analyzed in order to provide information on the nucleon-nucleus optical model potential. In particular, the energy dependence is being investigated, and comparison with existing proton elastic scattering data is expected to give precise information on the isospin-dependent part of the optical potential.

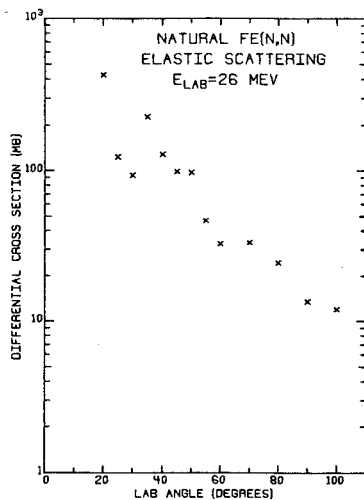


FIGURE 1

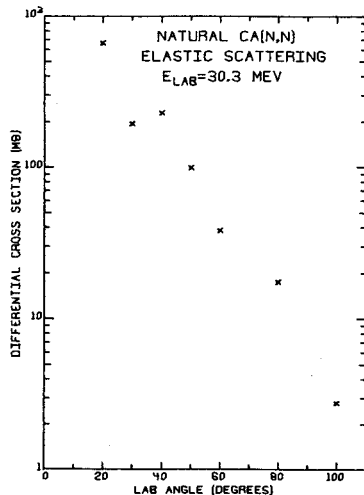


FIGURE 2

In the usual formulation of the optical model potential for nucleons,¹ neutrons and protons differ by terms dependent on the projectile energy and on the symmetry term, which is proportional to $(N-Z)/A$. By utilizing a $N=Z$ nucleus (^{40}Ca) the symmetry potential vanishes, making the analysis of the velocity dependence easier. This will be investigated by comparing data taken at various neutron energies. Where good proton data is available neutron energies are chosen such that both the neutron and proton have the same average velocity at the nucleus, that is, that $E_n = E_p - \bar{V}_c$, where \bar{V}_c is the average Coulomb potential energy felt by the proton. By using this "velocity matching" technique to compare proton and neutron data, this experiment will be sensitive to any breaking of charge symmetry in the nucleon-nucleus potential. The data should be sensitive enough to detect a change in the strength of the central potential consistent with the magnitude of charge symmetry breaking proposed by Negele.²

This experiment utilizes the reaction $^7\text{Li}(p,n)^7\text{Be}$ (0,0.429) as a neutron source. A neutron flux of about 10^7 n/cm²/sec can be obtained at the scattering sample. A 300 kg iron shield is positioned by remote control to prevent source neutrons from reaching the detector directly. Because a beam swinger is used to vary the scattering angle and the neutron detector is located in a room separate from the neutron source, good shielding is achieved. The region around the scattering sample that is visible to the detector is filled with Helium to minimize air scattering background.

A large area (84 cm x 13 cm) liquid scintillator (NE224) detector is used, which provides pulse-shape-discrimination (PSD) information as well as energy and time-of-flight output. The data is collected using a PDP 11/45 computer and a versatile program which allows up to eight TOF spectra with energy thresholds and PSD gates. Multiple scattering and geometrical effects from the finite size of the scattering sample (about 1 mole) are calculated with a Monte-Carlo program. A scintillator mounted on the swinger detects 180° neutrons from the Li target. This monitor detector allows compensation for changes in target thickness and can remove dependence on current integration. A third detector is used to independently trigger LED's in both the main and monitor detectors. These LED pulses are processed and independently counted to give the total dead time of the two detectors and to detect any gain shifts. This system gives reliable dead time corrections for dead times up to 50%.

1. G.R. Satchler, p. 389 of *Isospin in Nuclear Physics*; ed. D.H. Wilkinson (North Holland, 1972).
2. J.W. Negele, *Nucl. Phys. A165*, (1971) 305.

Elastic Scattering of ${}^6\text{Li}$ at 75 MeV

R. Huffman, A. Galonsky, and R.G. Markham

In this study we plan to measure ${}^6\text{Li}$ elastic scattering at 75 MeV for a wide range of targets. Similar data from other groups is now, or will soon be, available at both higher and lower energies on many of the same targets we plan to use. Hence, these studies will fill in a missing energy point and perhaps allow one to learn of the simultaneous mass and energy dependence of the optical model parameters for ${}^6\text{Li}$ elastic scattering.

To date, data have been obtained for small angles ($<30^\circ$) for targets of ${}^{90}\text{Zr}$, ${}^{124}\text{Sn}$ and ${}^{208}\text{Pb}$. For these measurements, a surface-barrier detector telescope and a single monitor detector were used on opposite sides of the beam. Monitor to charge ratios and right-left measurements were used to ensure proper beam alignment and stability. The telescope pulses and monitor pulses (with charge-integrator-triggered test pulses) were all processed in the same octal ADC and so were all subject to the same system dead-time. A preliminary analysis of the ${}^{90}\text{Zr}$ data has been carried out and is shown in Fig. 1. Past 10° the ratio σ/σ_R falls rapidly in an oscillatory but monotonic fashion.

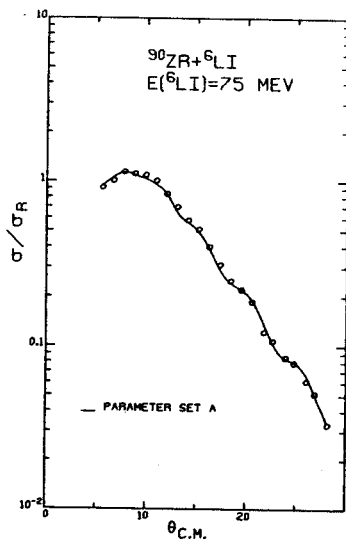


Fig. 1.--Elastic scattering data for ${}^{90}\text{Zr}({}^6\text{Li}, {}^6\text{Li})$ at an incident energy of 75 MeV. The curve is the result of model calculations using the parameter set A of Table I.

The optical model analyses are being carried out using the computer code SGIBELUMP. Both the real and imaginary potentials are volume potentials of the Woods-Saxon form. The geometry parameters as well as the well depths have been allowed to vary independently. The parameters from two equally good fits are listed in Table I and one of these fits is shown in Fig. 1. A plot of the other fit would be indistinguishable. A search for discrete families and for the continuous ambiguity has not been made.

Large angle data still need to be taken for the ${}^{90}\text{Zr}$, ${}^{124}\text{Sn}$, and ${}^{208}\text{Pb}$ targets and complete measurements are planned for targets of ${}^{28}\text{Si}$, ${}^{40}\text{Ca}$, and ${}^{58}\text{Ni}$.

Table I--Two sets of parameters from optical model analyses of scattering data of ${}^{90}\text{Zr}({}^6\text{Li}, {}^6\text{Li})$ at 75 MeV bombarding energy.

| Parameter Set | V_R (MeV) | r_R (Fm) | a_R (Fm) | V_I (MeV) | r_I (Fm) | a_I (Fm) |
|---------------|-------------|------------|------------|-------------|------------|------------|
| A | 241.93 | 1.296 | 0.688 | 13.905 | 1.724 | 0.879 |
| B | 106.152 | 1.443 | 0.655 | 13.905 | 1.719 | 0.909 |

Greenlees, Pyle, and Tang¹ pioneered the analysis of proton elastic scattering using an optical model formulated in terms of neutron and proton matter distributions. Recently, refinements in this approach have been described by Sinha and others.^{2,3,4} Through the Lane model of the optical potential

$$V = V_0 + \frac{4\bar{t} \cdot \bar{t}}{A} v_1 \quad (1)$$

it is possible to relate quasielastic scattering to the optical potential, where the isospin potential V_1 is responsible for the (p,n) reaction. The isospin potential V_1 in turn can be written approximately in terms of nuclear matter distributions. Schery *et al.*⁵ have used this approach in an effort to determine neutron matter distributions from the (p,n) reaction. The present project is an effort to more fully investigate the validity of this procedure.

The project involves developing refinements in the reaction models and obtaining high precision (p,n) data with which to test the models. Precision must be sufficient to reveal differences in angular distributions of scattering on nuclides in isotopic and isotonic sequences. We plan to obtain data on the tin isotopic sequence at 35 and 42 MeV proton energy and on the N=82 isotonic sequence at energies above 30 MeV. Preliminary data have been obtained for ¹²⁴Sn and ¹¹²Sn at 35 MeV. Additional high precision data on single nuclides may be necessary if existing data are found to be of insufficient quality.

In the development of the reaction models there are several important questions that need to be examined more fully. These include the need for a density dependence in the isospin component of the effective nucleon-nucleon interaction v_t , the incorporation of exchange effects into the model, and the development of an imaginary component W_1 in the isospin potential (also formulated in terms of neutron and proton matter distributions).

In analogy to the procedure reviewed by Sinha⁴ for the full optical potential, we have formulated the following semiclassical model for W_1 :

$$W_1(r) = \frac{\hbar}{4} v_p(r) (\bar{\sigma}_{pn}(r) \rho_n(r) - \bar{\sigma}_{pp}(r) \rho_p(r)) \quad (2)$$

where v_p is the velocity of the incident proton at position r in the nucleus and the $\bar{\sigma}_{ij}(r)$ are average nucleon-nucleon cross sections which take into account restrictions on excitations of bound nucleons due to the Pauli exclusion principle. Both the shape and strength of this potential well vary with projectile energy and target nucleus. Fig. 1 shows $V_1 = U_1 + iW_1$ evaluated for ¹²⁴Sn at proton energies of 23 and 35 MeV.

It can be seen that at a higher energy W_1 becomes both stronger and less surface peaked.

Equation (2) assumes zero range for the nucleon-nucleon interaction. For the full optical potential it was found important to include the effects of finite range in the imaginary term by replacing ρ_i with effective nucleon distributions obtained from folding a nucleon-nucleon interaction with ρ_i .⁴ We have found that a similar effect is important for W_1 . Fig. 2 shows a comparison of the predictions with preliminary ¹²⁴Sn(p,n)¹²⁴Sb data obtained at 35 MeV. The curves are DWBA calculations with the strength and neutron parameters of V_1 adjusted for best agreement with data. The full curve is the prediction of the basic real form for V_1 , the dotted curve in the prediction of a complex V_1 using zero range for W_1 , and the dashed curve is the prediction of a complex V_1 with the mean square range of ρ_n and ρ_p increased by 4.27 fm² (the range of v_t used in the calculation for V_0). The number of free parameters in all cases is the same. The use of a complex V_1 with finite range is seen to significantly improve the prediction of the data. A similar improvement was observed for ²⁰⁸Pb at proton energies of 25.8, 35.0, and 45.0 MeV.

*Moody College, Texas A&M University.

1. G.W. Greenlees, G.J. Pyle, and Y.E. Tang, Phys. Rev. 171, 1115(1968).
2. G.L. Thomas, B.C. Sinha, and F. Duggan Nucl. Phys. A203, 305(1973).
3. B. Sinha and F. Duggan, Nucl Phys. A226, 31(1974).
4. B. Sinha, Physics Reports 20, 1(1975).
5. S.D. Schery, D.A. Lind, and H. Wieman, Phys. Rev. C14, 1800(1976), and references therein.

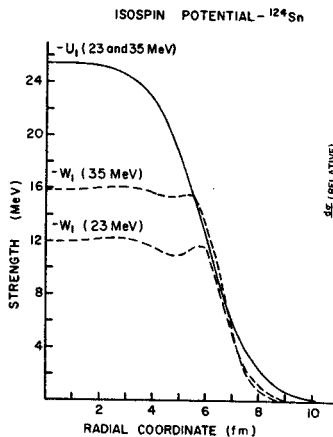


FIG. 1

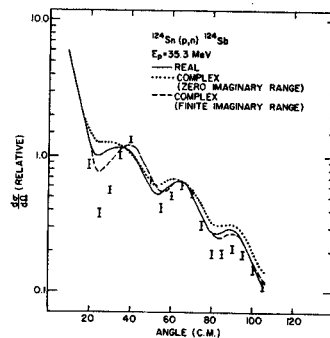


FIG. 2

An A-Dependence in the Optical Model for
Protons Below the Coulomb Barrier

Cleland Johnson* and Aaron Galonsky

Nothing can be learned about the optical potential from elastic scattering at energies well below the Coulomb barrier. Coulomb scattering overwhelms any nuclear effects. With respect to reaction cross sections the Coulomb intervention is different; penetration of its barrier is small, but what cross section results is purely nuclear and, in the optical model, is determined by the parameters of its complex potential. When neutron emission is energetically possible, it accounts for almost all of the cross section a few hundred keV above threshold and beyond. Hence, a measurement of the (p,n) cross section is essentially a measurement of the reaction cross section.

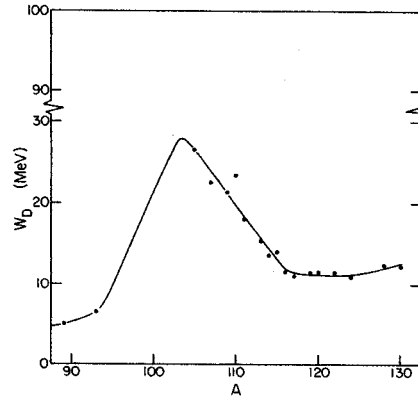
Many (p,n) excitation functions on medium-weight nuclei have been measured.¹ Dominated by the energy dependence of barrier penetrability, they are steeply rising functions. In the case of $^{116}\text{Cd}(p,n)$, for example, the cross section increases by a factor of 300 between 3 and 5 MeV.¹ It is customary and instructive to remove the Coulomb effect from an excitation function by dividing it by the Coulomb penetrability. The resulting function, dubbed strength function, is almost independent of proton bombarding energy. In this function nuclear effects are not masked.

One nuclear effect which should be seen is passage through some single-particle shell-model states. Around mass 120, for example, the proton 3p state has in fact been observed by this technique; it is seen to be unbound by ~ 6 MeV.² The Coulomb barrier, of course, makes such a state quasibound. The 3s proton state³ and both the 3s and 4s neutron states⁴ were detected earlier, so-called size resonances, not in excitation functions but in plots of strength function vs. A for a fixed nucleon bombarding energy. The neutron peaks around A=55 and 170 are rather famous.

In the detailed work around mass 120, i.e. work on (p,n) reactions in tin isotopes, a regularity was found in the location of the peak of the 3p resonance as a function of the mass, and, therefore, radius of the target tin isotope. With increasing mass the resonant energy decreased, just as one would expect. Furthermore, the excitation functions could well be fitted with a reasonable choice of optical-model parameters. The depth, W_D , of the imaginary well did have to be reduced by 30% from the value used with higher-energy data.

This type of analysis has now been extended to strength functions for 19 targets between ^{89}Y and ^{130}Te . The (p,n) data are old, some of them 20 years old, but the analysis is new, and the results are unexpected. To fit the data with the optical model requires that at least one parameter

change with target mass number. If only one parameter is to change, we have found that it must be W_D . The least-squares-fitted values are given in the figure. Interpretation of these results is under discussion. At the present time it seems certain that the usual spherical optical model with minor A dependencies will not work here.



* Oak Ridge National Laboratory.

1. C.H. Johnson, A. Galonsky, and C.N. Inskeep, ORNL-2910 (1960).
2. C.H. Johnson and R.L. Kernell, Phys. Rev. Letters 23, 20 (1969) and Phys. Rev. C 2 639 (1970) and C.H. Johnson, J.K. Bain, C.M. Jones, S.K. Penny, and D.W. Smith, Phys. Rev. C 15, 196 (1977).
3. J.P. Schiffer and L.L. Lee, Jr., Phys. Rev. 107, 640 (1957).
4. See, for example, Pierre Marmier and Eric Sheldon, Physics of Nuclei and Particles, Academic Press, 1970, Vol. II, p. 1182.